JCB Article

An anillin homologue, Mid2p, acts during fission yeast cytokinesis to organize the septin ring and promote cell separation

Joseph J. Tasto,[2] Jennifer L. Morrell,[1,2] and Kathleen L. Gould[1,2]

[1]Howard Hughes Medical Institute and [2]Department of Cell and Developmental Biology, Vanderbilt University School of Medicine, Nashville, TN 37232

Anillin is a conserved protein required for cell division (Field, C.M., and B.M. Alberts. 1995. *J. Cell Biol.* 131:165–178; Oegema, K., M.S. Savoian, T.J. Mitchison, and C.M. Field. 2000. *J. Cell Biol.* 150:539–552). One fission yeast homologue of anillin, Mid1p, is necessary for the proper placement of the division site within the cell (Chang, F., A. Woollard, and P. Nurse. 1996. *J. Cell Sci.* 109(Pt 1):131–142; Sohrmann, M., C. Fankhauser, C. Brodbeck, and V. Simanis. 1996. *Genes Dev.* 10:2707–2719). Here, we identify and characterize a second fission yeast anillin homologue, Mid2p, which is not orthologous with Mid1p. Mid2p localizes as a single ring in the middle of the cell after anaphase in a septin- and actin-dependent manner and splits into two rings during septation. Mid2p colocalizes with septins, and *mid2Δ* cells display disorganized, diffuse septin rings and a cell separation defect similar to septin deletion strains. *mid2* gene expression and protein levels fluctuate during the cell cycle in a *sep1*- and Skp1/Cdc53/F-box (SCF)–dependent manner, respectively, implying that Mid2p activity must be carefully regulated. Overproduction of Mid2p depolarizes cell growth and affects the organization of both the septin and actin cytoskeletons. In the presence of a nondegradable Mid2p fragment, the septin ring is stabilized and cell cycle progression is delayed. These results suggest that Mid2p influences septin ring organization at the site of cell division and its turnover might normally be required to permit septin ring disassembly.

Introduction

Cytokinesis is the final stage of mitosis, during which a cell is irreversibly split into two daughters. In many eukaryotic organisms, an essential element of this process is an actomyosin-based contractile ring whose constriction is required to generate the force necessary to complete cell division. The genetically tractable yeast *Schizosaccharomyces pombe* is an excellent organism for studying cytokinesis, as it divides by medial fission after assembly and contraction of an actomyosin ring (for review see Feierbach and Chang, 2001). Based on the isolation and characterization of numerous mutants, the process of cell division in *S. pombe* can be divided into several steps.

The initial phase of cytokinesis involves establishing the division site at the center of a symmetrical cell. This process begins at the onset of mitosis when components of the contractile ring are recruited to the cell cortex immediately adjacent to the nucleus (for review see Chang, 2001). The proper localization of these medial ring components depends on Mid1p (Chang et al., 1996; Sohrmann et al., 1996). The next steps of cytokinesis, medial ring constriction and septation, require a conserved signaling cascade, referred to as the septation initiation network, that is organized at the spindle pole body, a microtubule organizing center analogous to the mammalian centrosome (for review see McCollum and Gould, 2001; Pereira and Schiebel, 2001). Septation occurs concomitantly with medial ring constriction as the primary septum is laid down in a centripetal manner behind the constricting actomyosin-based ring, which is then flanked on each side by secondary septa (for review see Le Goff et al., 1999). Physical separation of the two daughter cells is achieved, in part, through the degradation of the primary septum, although the mechanistic details of this process remain obscure.

In *S. pombe*, septins are clearly required for normal cell separation because deletion of septin genes expressed during vegetative growth generates a nonlethal chained cell phenotype (J. Pringle, personal communication; Longtine et al., 1996). Septins are a group of conserved GTPases originally

The online version of this article includes supplemental material.

Address correspondence to Kathleen L. Gould, Vanderbilt University School of Medicine, Department of Cell and Developmental Biology, B2309 MCN, 1161 21st Ave. South, Nashville, TN 37232. Tel.: (615) 343-9502. Fax: (615) 343-0723. E-mail: kathy.gould@vanderbilt.edu

Key words: *S. pombe*; cytokinesis; cell cycle; septin; mid2

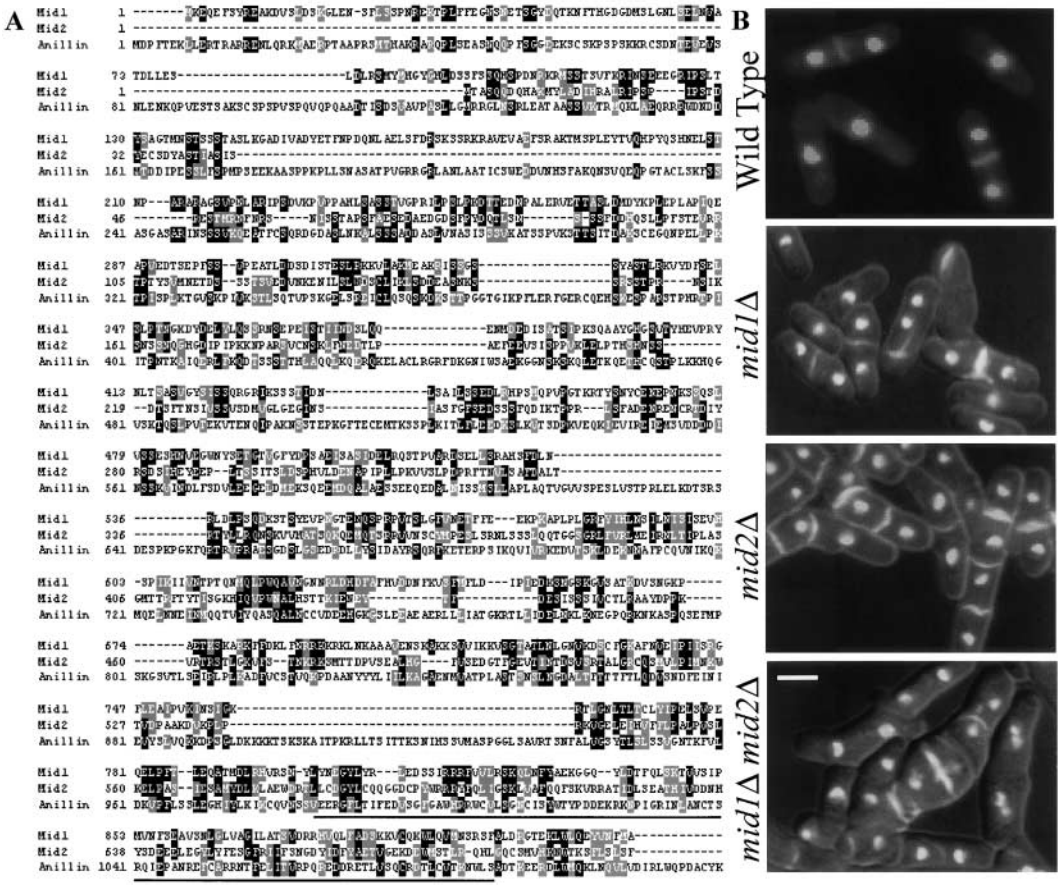

Figure 1. **Mid2p is an *S. pombe* anillin homologue.** (A) Alignment of human anillin with *S. pombe* Mid1p and Mid2p. Identical amino acids are in solid boxes and similar residues are shaded. The PH domain is underlined. (B) *mid2* is not essential. Wild type (KGY246), *mid1Δ* (KGY2955), *mid2Δ* (KGY3135), and *mid1Δ mid2Δ* (KGY3125) cells were grown at 25°C and stained with Hoechst 33258 and aniline blue. Bar, 5 μm.

identified in budding yeast (Hartwell, 1971) and now described in many organisms (for review see Faty et al., 2002; Macara et al., 2002). In *Saccharomyces cerevisiae*, septins are thought to perform multiple functions at the mother–daughter bud neck, such as providing a boundary that restricts certain determinants to particular cortical domains (for review see Faty et al., 2002) and acting as a scaffold necessary for the proper localization of many factors involved in polarity and cell division (for review see Gladfelter et al., 2001). Whether septins perform all of these roles in other organisms has yet to be established. However, most septins studied to date localize to the site of cell division, and disruption of septin function leads to cytokinesis defects in many cell types (Hartwell, 1971; Neufeld and Rubin, 1994; Longtine et al., 1996; Kinoshita et al., 1997).

One factor important for septin organization is the conserved protein anillin, which is concentrated in the cleavage furrow of dividing cells where it links the actin and septin cytoskeletons (Field and Alberts, 1995; Oegema et al., 2000; Kinoshita et al., 2002). Further, the disruption of anillin function leads to defects in cytokinesis (Oegema et al., 2000). In *S. pombe*, there is no evidence that the one described anillin homologue, Mid1p, interacts with the septin cytoskeleton. Rather, the loss of Mid1p function results in misplaced actomyosin rings and septa (Chang et al., 1996; Sohrmann et al., 1996; Bahler et al., 1998a; Paoletti and Chang, 2000), whereas a septin deletion results in a cell separation defect (J. Pringle, personal communication; Longtine et al., 1996). Thus, these proteins appear to be involved in different stages of cell division.

Examination of the recently completed *S. pombe* genome sequence indicated the presence of a second ORF with significant homology to Hs anillin and mid1 that we have termed mid2 (Q9P7Y8 or SPAPYUG7.03C). In this study, we have examined the functional relationship of Mid2p with both Mid1p and the septins. Mid2p is regulated in abundance during the cell cycle, and we have examined the reasons for its periodicity. Our results suggest that Mid2p plays a role during late mitosis in organizing the septin ring and that Mid2p degradation may facilitate septin ring disassembly.

Results

S. pombe mid2 encodes a second anillin homologue

Examination of the *S. pombe* protein database identified an uncharacterized protein with homology to Mid1p that has been termed Mid2p (Q9P7Y8) (Fig. 1 A). Mid2p has a predicted molecular mass of 78.7 kD. The overall similarity between Mid2p and either Mid1p or Hs anillin is 24.3% and 19.5%, respectively. Mid2p also shares moderate sequence similarity with two other fungal proteins, *S. cerevisiae* Bud4p (14.9%; Sanders and Herskowitz, 1996) and *Candida albi-*

cans Int1p (12.8%; Gale et al., 1996). All of these proteins possess a carboxy-terminal pleckstrin homology (PH)* domain while Mid2p has the shortest amino terminus (Fig. 1 A) (Lemmon and Ferguson, 2001).

Sporulation and tetrad dissection of diploids that were confirmed to have the entire *mid2* ORF successfully replaced by *ura4*$^+$ produced four viable colonies, indicating that *mid2* is not essential for viability. In contrast to the misplaced septum phenotype observed in *mid1Δ* cells, the loss of *mid2* produced "chained" cells in which repeated rounds of nuclear division and septum synthesis occurred with delayed cell separation (Fig. 1 B). To determine if Mid1p and Mid2p share an overlapping essential function, a *mid1Δ mid2Δ* strain was constructed. This strain was viable at 25°C, exhibited both septum placement and cell separation defects (Fig. 1 B), and was temperature sensitive (unpublished data), as is the *mid1Δ* strain alone. Combined with the fact that both Mid1p–GFP and Mid2p–GFP were able to localize properly in the absence of the other (unpublished data), we conclude that *mid1* and *mid2* are not functionally redundant.

Mid2p localization and abundance are cell cycle regulated

To better understand the role of Mid2p in cell separation, its subcellular localization was examined. A carboxy-terminal Mid2p–GFP fusion protein was constructed by homologous recombination at the endogenous locus of *mid2*$^+$ in order to maintain its physiological expression level. Mid2p–GFP localized to the medial region in 17% of the cells in an asynchronous population (Fig. 2 A). Using time-lapse microscopy, Mid2p–GFP was observed to initially form a single ring, split into two rings as the septum formed, and then disappear as cells separated (see Video 1, available at http://www.jcb.org/cgi/content/full/jcb.200211126/DC1). Mid2p–GFP was stable to a variety of fixation procedures, thereby permitting it to be visualized in fixed cells also stained with DAPI and antibodies to tubulin. In this case, Mid2p was only detected at the ring in late anaphase cells that lacked spindles (Fig. 2 B; unpublished data).

Because Mid2p–GFP localization was transient, we asked whether Mid2p levels were cell cycle regulated. A Mid2p–HA strain was constructed and used to examine protein levels in a culture synchronized by centrifugal elutriation. Mid2p–HA levels fluctuated considerably as cells traversed the cell cycle, peaking concomitantly with septation (Fig. 2 C). Also, Mid2p–HA appeared to migrate as several distinct species (Fig. 2 C). These multiple isoforms are due to phosphorylation because treatment of immunoprecipitated Mid2p–HA with λ-phosphatase collapsed them into a single, faster-migrating species (Fig. 2 D).

To determine if Mid2p periodicity was due, at least in part, to fluctuations in its mRNA, *mid2* transcript levels were monitored from a synchronous culture of wild-type cells harvested by centrifugal elutriation. *mid2* mRNA levels did vary significantly during vegetative growth, peaking as cells entered mitosis (Fig. 2 E).

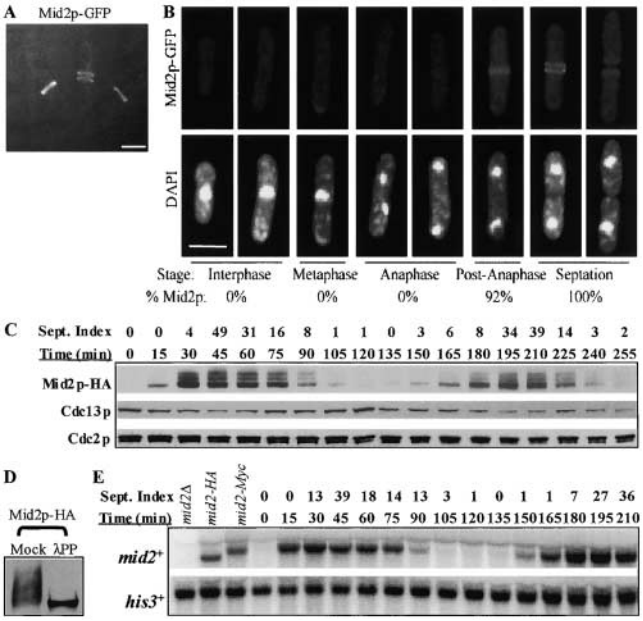

Figure 2. **Cell cycle regulation of Mid2p.** (A) Localization of Mid2p–GFP in live cells (KGY2422) (see Video 1, available at http://www.jcb.org/cgi/content/full/jcb.200211126/DC1). (B) *mid2–GFP* cells were fixed with ethanol and stained with DAPI to visualize DNA. At least 70 cells from each cell cycle stage (as determined by microtubule staining) were counted to determine the percentage of cells, indicated below the images, with a medial Mid2p–GFP signal. Representative images of each stage are shown. (C and E) *mid2–HA* (KGY2843) and wild-type (KGY246) cells were grown to mid-log phase, and cultures synchronized in G2 were obtained by centrifugal elutriation. Cell samples were collected at the indicated times after synchronization and processed for protein (C) or RNA (E). (C) Cell cycle progression was monitored by determining septation index and Cdc13p levels. Mid2p–HA, Cdc13p, and Cdc2p (which served as a loading control in all of our immunoblots) were detected by immunoblotting with 12CA5, anti-Cdc13p, and anti-PSTAIR antibodies, respectively. (D) Mid2p–HA (KGY2843) was immunoprecipitated with 12CA5 antibodies and incubated with λ-phosphatase or mock treated. (E) Northern analysis of *mid2* transcripts from asynchronous cultures of *mid2Δ* (KGY3135), *mid2–HA* (KGY2843), and *mid2–myc* (KGY2432) strains and a synchronized culture of wild-type cells (KGY246). Cell synchrony was monitored by septation index. *his3* mRNA served as a loading control. Bars, 5 μm.

Mid2p is destroyed by Skp1/Cdc53/F-box (SCF)–dependent proteolysis

Because of the dynamic changes in Mid2p–HA levels during the cell cycle (Fig. 2 C), we tested if Mid2p was targeted for destruction by ubiquitin-mediated proteolysis. First, we examined whether Mid2p was ubiquitinated in vivo. In an *mts3-1* mutant strain, multi-ubiquitinated conjugates accumulate at the restrictive temperature due to the abrogation of proteosome function (Gordon et al., 1996). Therefore, polyubiquitinated Mid2p–Myc would be expected to accrue in an *mts3-1* strain, but only if the relevant E3 ubiquitin ligase was active. *S. pombe* securin, Cut2p, was used as a positive control for a ubiquitin-conjugated protein (Berry et al., 1999). Both Cut2p–Myc and Mid2p–Myc were readily de-

*Abbreviations used in this paper: APC, anaphase-promoting complex; LatA, latrunculin A; PEST, Pro/Glu/Ser/Thr; PH, pleckstrin homology; SCF, Skp1/Cdc53/F-box.

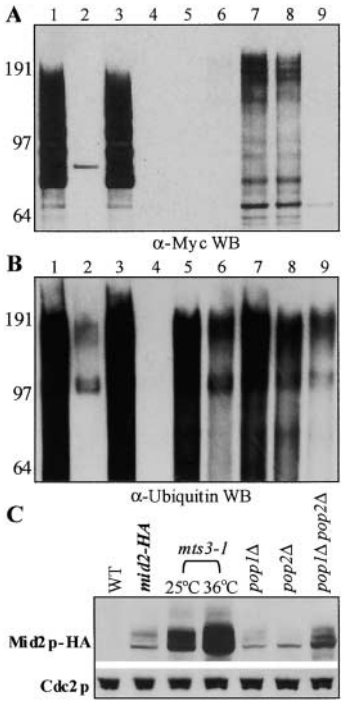

Figure 3. **Mid2p is regulated by SCF-dependent proteolysis.** (A and B) In vivo ubiquitination assays. The *cut2–myc mts3-1* (KGY1923) (lane 1), *cut2–myc mts3-1 lid1-6* (KGY1948) (lane 2), *cut2–myc mts3-1 skp1-A4* (KGY4050) (lane 3), *mts3-1* (KGY574) (lane 5), *mid2–myc* (KGY2432) (lane 6), *mid2–myc mts3-1* (KGY3687) (lane 7), *mid2–myc mts3-1 lid1-6* (KGY1977) (lane 8), and *mid2–myc mts3-1 skp1-A4* (KGY1978) (lane 9) strains containing pREP1-His_6–ubiquitin (Ub) and the *mid2-myc mts3-1* strain (KGY3687) without vector (lane 4) were grown at 25°C for 22 h in the absence of thiamine to induce His_6–Ub expression and then shifted to 36°C for 4 h. Ub-conjugated proteins were isolated and immunoblotted for either Myc (A) or Ub (B). (C) Denatured protein lysates from wild-type (KGY246), *mid2–HA*(KGY2843), *mid2–HA mts3-1*(KGY3307), *pop1Δ mid2–HA* (KGY3702), *pop2Δ mid2–HA* (KGY3699), and *mid2–HA pop1Δ pop2Δ* (KGY3700) strains were immunoblotted with anti-HA (12CA5) to detect Mid2p–HA and anti-PSTAIR to detect Cdc2p.

tected as multi-ubiquitinated proteins in isolates of ubiquitin-conjugated proteins from an *mts3-1* strain overproducing tagged ubiquitin (Fig. 3 A, lanes 1 and 7).

Two ubiquitin ligases that participate in cell cycle–regulated proteolysis are the anaphase-promoting complex (APC) and the Skp1/Cdc53/F-box (SCF) (Willems et al., 1999; Zachariae and Nasmyth, 1999). To determine if either of these E3 ligases were responsible for Mid2p–Myc ubiquitination, we took advantage of available conditional lethal mutations that disrupt the function of each. Lid1p is a component of the APC that acts during mitosis and G1 (Peters, 2002), and a *lid1-6* mutation prevents APC function at the restrictive temperature (Berry et al., 1999). Skp1p is a core member of the SCF complex, an E3 required for G1/S progression (Kominami et al., 1998; Krek, 1998; Willems et al., 1999), and the *skp1-A4* allele abrogates SCF activity at 36°C (Yamano et al., 2000). Whereas the ubiquitination of Cut2p–Myc relied upon an active APC (Fig. 3 A, lanes 1 and 2), Mid2p–Myc did not (Fig. 3 A, lanes 7 and 8). Rather, Mid2p–Myc ubiquitination was strictly dependent upon functional Skp1p (Fig. 3 A, lanes 7 and 9), whereas Cut2p–Myc proteolysis was SCF independent (Fig. 3 A, lanes 1 and 3). An anti-ubiquitin immunoblot confirmed that ubiquitin conjugates were purified in all strains except the one lacking the His–ubiquitin vector (Fig. 3 B).

Consistent with the in vivo ubiquitination assay data, Mid2p–HA levels accumulated in an *mts3-1* strain (Fig. 3 C) but not in an APC mutant at the restrictive temperature (unpublished data). Mid2p–HA abundance was also elevated in cells lacking two F-box–encoding genes, *pop1* and *pop2*, components of SCF ubiquitin ligases (Fig. 3 C) (Kominami et al., 1998). Taken together, these results are consistent with the hypothesis that Mid2p is destroyed by SCF-dependent ubiquitination in vivo.

mid2 expression is dependent on the forkhead-like transcription factor *sep1*

The fact that *mid2* mRNA levels oscillate during vegetative growth (Fig. 2 E), coupled with the observation that the *mid2Δ* cell separation defect resembles the loss of a putative transcription factor, *sep1* (Fig. 4 A; Ribar et al., 1999), prompted us to examine whether *mid2* transcript abundance depended on Sep1p function. A *cdc25-22* block and release synchronization protocol (Moreno et al., 1990) was used to address this question because the *sep1Δ* strain cannot be syn-

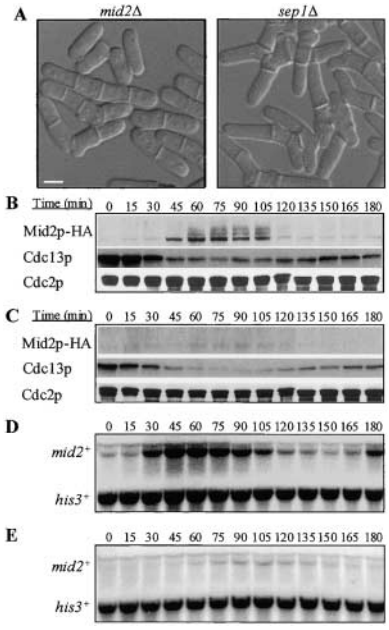

Figure 4. ***mid2* expression depends on Sep1p.** (A) Differential interference contrast images of *mid2Δ* (KGY3135) and *sep1Δ* (KGY3419) cells grown in YE medium at 32°C. Bar, 5 μm. (B–E) *cdc25-22 mid2–HA* (KGY3306) (B and D) and *cdc25-22 mid2–HA sep1Δ* (KGY3457) (C and E) cells were arrested in G2 by shift to 36°C for 4 h. Cultures were then released to 25°C and cell pellets collected at the indicated times to analyze Mid2p–HA and $mid2^+$ transcript levels. (B and C) Mid2p–HA and Cdc2p levels were determined by immunoblotting with 12CA5 and anti-PSTAIR, respectively. Mitotic progression was determined by assaying Cdc13p fluctuations by immunoblotting. (D and E) Northern blot analysis of *mid2* transcript levels from the same time points analyzed in B and C. The *his3* transcript served as a loading control.

chronized by centrifugal elutriation due to its chained cell phenotype (Ribar et al., 1999). In these cells, progression through mitosis was monitored by examining fluctuations in Cdc13p–cyclin B levels that occur during this period (Alfa et al., 1989). Although readily detectable in *cdc25-22* cells proceeding through mitosis (Fig. 4 B), Mid2p–HA levels were clearly diminished in *sep1Δ* cells during the same time course (Fig. 4 C). The drop in Mid2p levels correlated with a significant decrease in *mid2* mRNA abundance in the absence of *sep1,* although delayed and reduced amounts of the *mid2* transcript were detected (Fig. 4, D and E). These results indicate that Sep1p plays an important role in setting Mid2p levels.

To address whether $mid2^+$ might be the critical target of Sep1p, we tested whether expression of $mid2^+$ from a heterologous promoter was able to suppress the cell separation defect of a *sep1Δ* strain. At best, we observed a partial rescue (unpublished data), indicating that other targets of Sep1p must exist that, together with Mid2p, are required for efficient cell separation in *S. pombe*.

Medial ring localization of Mid2p–GFP requires F-actin

To determine if Mid2p required F-actin for its association with the medial ring, Mid2p–GFP localization was monitored in cells released from a *cdc25-22* block into either DMSO or latrunculin A (LatA), which promotes F-actin depolymerization (Ayscough et al., 1997). In control cells, the first Mid2p–GFP rings appeared at 60 min and persisted (Fig. 5 A; unpublished data). In contrast, the LatA-treated cells failed to form Mid2p–GFP rings even after 150 min (Fig. 5 A). In an asynchronous culture of cells, however, Mid2p–GFP persisted at the medial ring 15 min after LatA addition (Fig. 5 B), suggesting that once recruited, Mid2p's association with the medial ring is actin independent.

Mid2p is required for proper septin ring organization

Because the loss of *mid2* produced a strikingly similar phenotype to that of the *spn4Δ* mutant (Fig. 5 C) (J. Pringle, personal communication; Longtine et al., 1996), and the phenotype of a *mid2Δ spn4Δ* double mutant strain was similar to either single mutant (Fig. 5 C), it seemed likely that Mid2p and septins were involved in the same step of cell division. We therefore examined if Mid2p depended upon septins for its medial ring association. In *spn4Δ* cells, Mid2p–GFP was expressed (unpublished data) but failed to localize to the medial ring and was instead distributed throughout the cytoplasm (Fig. 5 D). We next determined whether or not septins and Mid2p colocalized. Images taken from a strain expressing endogenously tagged Mid2p–GFP and Spn1p–CFP show that their localization patterns are indistinguishable (Fig. 6 A). We also tested whether septin localization was affected by the lack of Mid2p function. To perform this experiment, the *spn3* locus was modified to encode an Spn3p–GFP fusion protein. This strain was morphologically wild type, implying that the epitope does not disrupt septin function. By time-lapse microscopy, Spn3–GFP was observed to form a single ring, then form two rings, and finally disperse upon the completion of cell separation (Fig. 6 B; see Video 2, available at http://www.jcb.org/cgi/content/full/jcb.200211126/DC1). In a

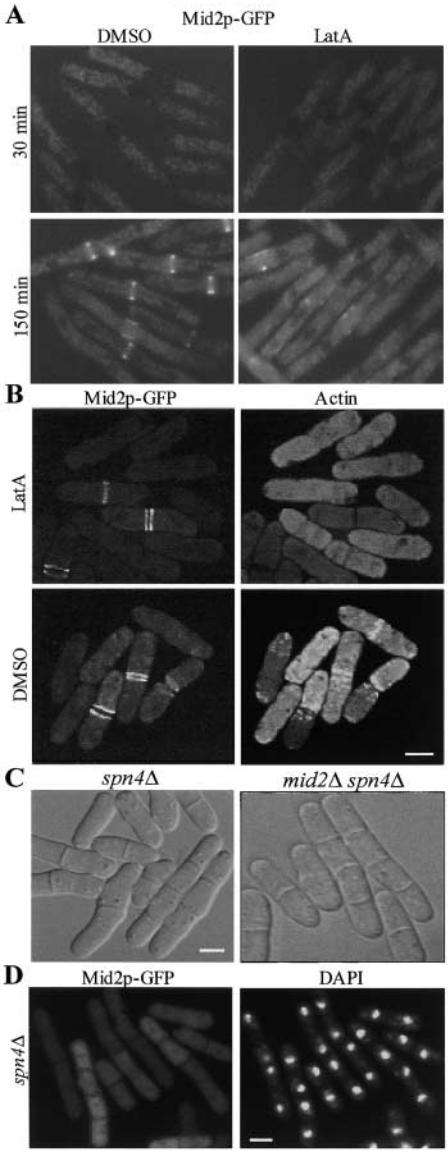

Figure 5. **Mid2p localization requires F-actin and septins.** (A) *cdc25-22 mid2–GFP* cells (KGY3123) were grown to mid-log phase at 25°C, shifted to 36°C for 4 h, and released to 25°C in either DMSO or 100 μM LatA. Images of live cells at the indicated times are presented. (B) Asynchronously growing *mid2–GFP* cells (KGY2422) were treated with DMSO or 200 μM LatA for 15 min and fixed with formaldehyde. The actin cytoskeleton was visualized with AlexaFluor®594-phalloidin. (C) Differential interference contrast images of *spn4Δ* (KGY3986) or *mid2Δ spn4Δ* (KGY4356) grown in YE medium at 32°C. (D) *mid2–GFP spn4Δ* cells (KGY4217) were grown at 32°C, fixed with ethanol, and stained with DAPI. Bars, 5 μm.

mid2Δ strain, Spn3p–GFP was recruited to the site of cell division in a loosely organized ring and then appeared to spread bilaterally across the septum as a disc over time (Fig. 6 C; see Video 3, available at http://www.jcb.org/cgi/content/full/jcb.200211126/DC1).

Because septa persist in a *mid2Δ* strain, we wondered whether the abnormal Spn3p–GFP localization was a direct consequence of the loss of *mid2* or a byproduct of the cell separation defect in these cells. Therefore, we examined Spn3p–GFP localization in a different mutant that also displays multiple uncleaved septa. In the calcineurin deletion,

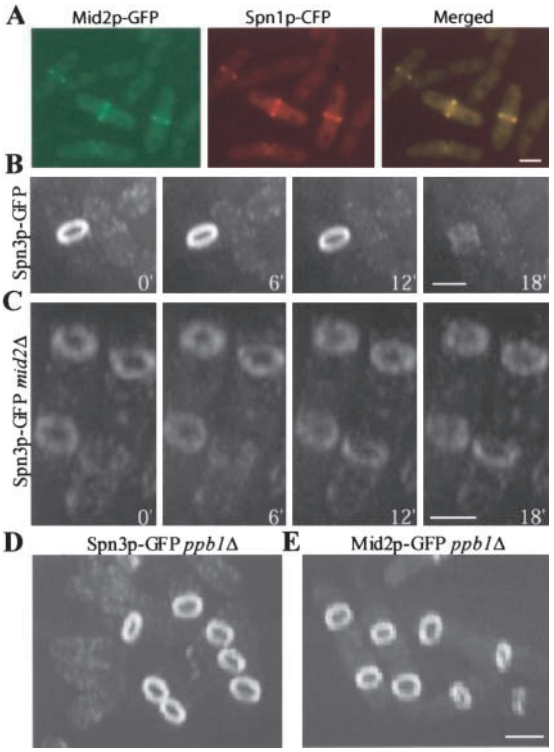

Figure 6. **Mid2p is required for septin ring organization.** (A) Cells producing both Mid2p–GFP and Spn1p–CFP (KGY3295) were imaged separately using a YFP/CFP filter set, and these images were also merged. (B) Time-lapse images of Spn3p–GFP in a wild-type background (KGY3244; see Video 2, available at http://www.jcb.org/cgi/content/full/jcb.200211126/DC1). (C) Time-lapse images of Spn3p–GFP in a *mid2Δ* strain background (KGY3304; see Video 3). (D) Spn3p–GFP (KGY4220) and (E) Mid2p–GFP (KGY4216) were visualized in live *ppb1Δ* cells. Bars, 5 μm.

ppb1Δ, which displays this phenotype (Yoshida et al., 1994), Spn3–GFP assembled into tight rings at the cell cortex (Fig. 6 D), as did Mid2p–GFP (Fig. 6 E). This observation indicates that septin rings are not necessarily disorganized in cell separation mutants but are specifically affected by the absence of Mid2p.

Delineation of Mid2p functional domains

To determine which regions of the protein dictated Mid2p localization and were important for its function, a series of *mid2* constructs were generated and tested for their ability to rescue the *mid2Δ* cell separation defect, their localization pattern, and any overexpression phenotype (Fig. 7 B). Immunoblot analysis of anti-HA immunoprecipitations from denatured lysates confirmed that these fragments were all produced (Fig. 7 C).

The PH domain of Mid2p encompasses amino acids 582–685 (Fig. 7 A). A construct lacking most of this motif (Mid2p 1–595) does not rescue the *mid2Δ* phenotype or localize to the medial ring. However, two constructs containing the PH domain (Mid2p 569–704 and Mid2p 596–704) failed to direct GFP to the medial ring or rescue the null phenotype (Fig. 7 B; unpublished data). Therefore, the PH domain appears to be necessary, but not sufficient, for Mid2p localization and function. Indeed, the smallest fragment directing medial ring localization was Mid2p (336–704) (Fig. 7 D), although it also seemed to concentrate in or around the nucleus. Mid2p (336–704) was also able to partially rescue the *mid2Δ* phenotype.

In contrast to the denatured lysates analyzed directly in Fig. 2 C and Fig. 4 B, we noticed that HA–Mid2p was degraded during an immunoprecipitation procedure to produce a variety of smaller fragments (Fig. 7 C). However, deletion of the Mid2p amino terminus, which contains three putative PEST (Pro/Glu/Ser/Thr) domains that are predicted to contribute to protein instability by facilitating ubiquitin-mediated proteolysis (Rogers et al., 1986), largely prevented this degradation (Fig. 7 C). Coupled with the fact that Mid2p is multi-ubiquitinated in vivo (Fig. 3 A), these

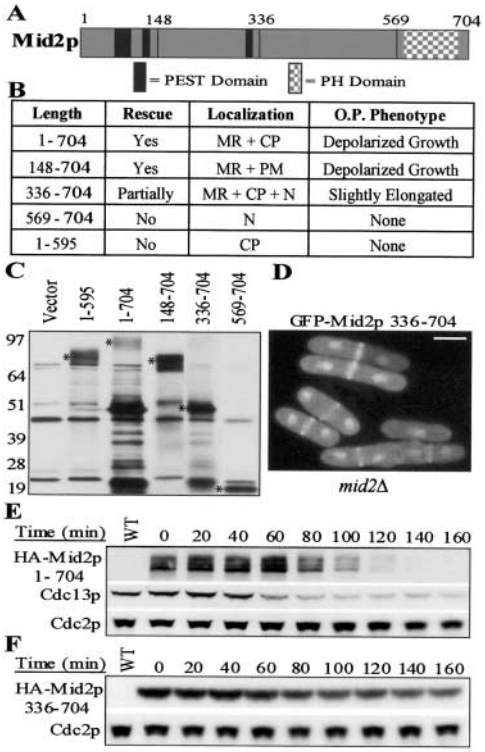

Figure 7. **Mid2p functional domains.** (A) Diagram of full-length Mid2p depicting the PEST and PH domains. The fine vertical lines indicate the positions of amino acids 148, 336, and 569. (B) The ability of HA– or GFP–Mid2 fusion proteins produced from the *nmt41* promoter to rescue the *mid2Δ* (KGY3135) phenotype, their localization pattern in KGY3135, and the overproduction phenotype of untagged constructs when expressed from the full-strength *nmt1* promoter in wild-type cells (KGY246). MR, medial ring; CP, cytoplasmic; PM, plasma membrane; N, nuclear; O.P., overproduction. (C) Wild-type cells expressing the indicated fragments were lysed under denaturing conditions, and the lysates were subjected to an anti-HA immunoprecipitation and then immunoblotted. An asterisk indicates the expected size of a fusion protein. Bands not present in vector control lane are degradation products. (D) Image of live *mid2Δ* cells expressing GFP–Mid2p(336–704) under control of the derepressed *nmt41* promoter. Bar, 5 μm. (E and F) A *cdc25-22 mid2Δ* strain (KGY4062) containing either (E) pREP41HA–Mid2p(1–704) or (F) pREP41HA–Mid2p(336–704) was grown for 22 h in the absence of thiamine at 25°C, shifted to 36°C for 4 h, and then released to 25°C in the presence of excess thiamine while time points were collected every 20 min for immunoblot analysis. HA–Mid2p and Cdc2p levels were determined by immunoblotting with 12CA5 and PSTAIR, respectively. Mitotic progression was determined by assaying for Cdc13p fluctuations by immunoblotting.

observations suggest that the putative PEST domains contribute to Mid2p instability.

To test whether deletion of the PEST motifs would yield a stable version of Mid2p, either full-length Mid2p or Mid2p (336–704) was produced in *mid2Δ cdc25-22* cells under control of the moderate *nmt41* promoter as amino-terminal HA fusion proteins. After 22 h at 25°C in the absence of thiamine, these cells were shifted to 36°C to block cells at G2/M before maximal expression was reached. The cells were then released to 25°C in the presence of thiamine to prevent further transcription, and samples were taken periodically for immunoblot analysis. As with endogenous Mid2p, the full-length fusion protein was degraded as cells septated and began a new cell cycle (Fig. 7 E). In contrast, Mid2p (336–704) remained unmodified and significantly more stable (Fig. 7 F).

Overproduction of Mid2p leads to ectopic septin structures

Given that *mid2Δ* cells had disorganized septin rings, we tested if excess amounts of wild type or the stable form of Mid2p would affect the septin cytoskeleton. Cells overproducing full-length Mid2p from the strong *nmt1* promoter grew very slowly, became rounded, and had depolarized actin patches (Fig. 8 A), but did form colonies (unpublished data). In these cells, Spn3p–GFP was detected in aberrant filamentous structures that lacked F-actin, and very few cells were observed undergoing cytokinesis (Fig. 8 A). Overproduction of stable Mid2p (amino acids 336–704; Fig. 7 F) produced slightly elongated, rather than depolarized, cells that also grew very slowly (Fig. 8 A; unpublished data). In this case, septin rings did not disassemble on schedule. Instead, septin rings persisted at the new ends of cells well into the next cell cycle, and prominent remnants of septin structures could even be detected into a third cell division because they were observed at both tips in addition to the middle of the cell (Fig. 8 A).

To quantify this effect, five patterns of Spn3p–GFP localization were examined (Fig. 8 B). Septins are normally observed diffusely at the tips of interphase cells, but for the purpose of this quantification, tip localization was only considered if it was of equal intensity to the ring fluorescence. In the vector control, 83% of cells lacked Spn3p–GFP staining at the ring or tips while 17% of the cells contained a septin ring(s) at the center of the cell (n = 2,372 cells; Fig. 8 B, 1 and 2). By comparison, in the presence of stable Mid2p (336–704), the number of cells lacking Spn3p–GFP staining dropped to 33% while cells with only medial ring staining dropped to 9% (n = 1,982 cells; Fig. 8 B, 1 and 2). When Mid2p (336–704) was overproduced, the most prevalent pattern of Spn3p–GFP fluorescence was at one or both ends (32%; Fig. 8 B, 3). A small percentage of cells, 7%, exhibited Spn3p–GFP localization at the center of the cell in addition to the tips, implying that septin structures had persisted during one to two extra cell divisions (Fig. 8 B, 4). Finally, 19% of the cells overproducing Mid2p (336–704) had depolarized septin patches distributed throughout the cell (Fig. 8 B, 5). These three phenotypes were rarely observed in the vector control cells (<0.5%; Fig. 8 B, 3–5). Taken together, these data suggest that the carboxy terminus of Mid2p stabilizes septin ring structures and that the timely destruction of Mid2p facilitates the disassembly of septin rings normally observed during each cell cycle.

Discussion

In this study, we have characterized a novel *S. pombe* protein, Mid2p, related to the cell division site placement factor, Mid1p. Our results suggest that Mid2p is involved in the establishment of the septin ring that permits efficient cell

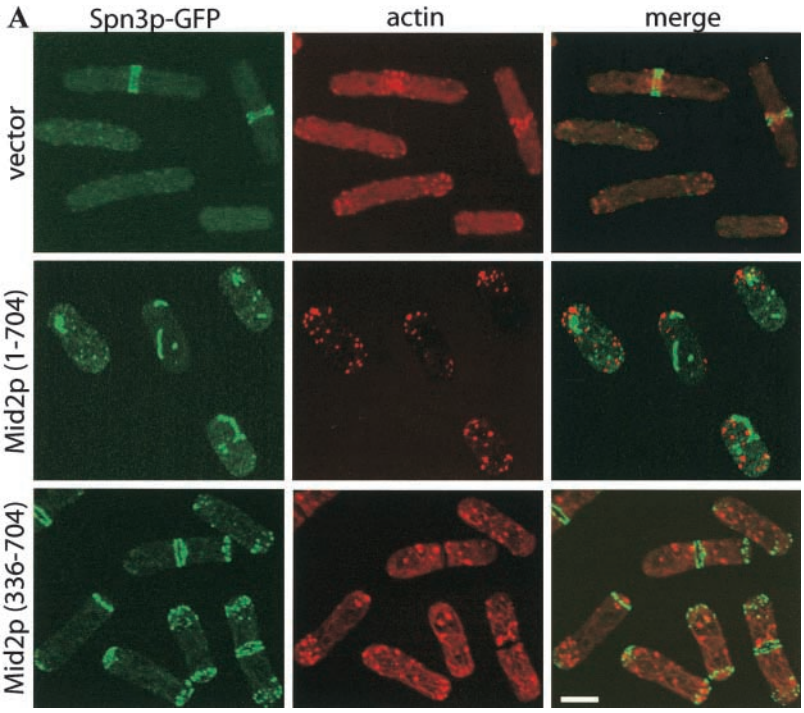

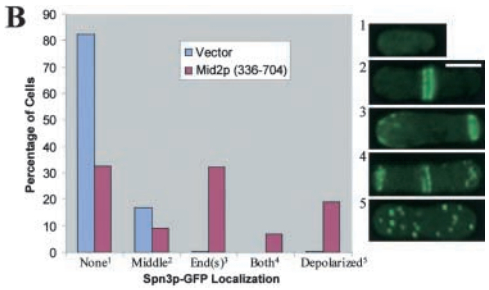

Figure 8. **Septin ring disassembly is delayed by the presence of nondegradable Mid2p.** (A) Spn3p–GFP cells (KGY3244) expressing high levels of Mid2p (1–704) or Mid2p (336–704) driven by the *nmt1* promoter were fixed with formaldehyde and stained with AlexaFluor®594-phalloidin. Images of actin and Spn3p–GFP were taken separately and also merged. (B) Spn3p–GFP cells expressing high levels of Mid2p (336–704) were fixed in ethanol and the following septin localization patterns were quantified in ~2,000 cells and compared with cells containing empty vector: None[1]; Middle[2]; End(s)[3]; Both[4]; or Depolarized[5]. Bars, 5 μm.

separation. Moreover, Mid2p degradation may facilitate septin ring disassembly.

Although our data indicate that both Mid1p and Mid2p act during cell division, it appears that their functions are nonoverlapping. There was no synthetic lethality observed in a double deletion strain, only an additive phenotype. Further, Mid1p localized appropriately in the absence of Mid2p and vice versa (unpublished data). Primary amino acid sequence and structure/function analyses also revealed some differences between these proteins. For instance, Mid1p possesses a nuclear localization signal and a large amino-terminal extension not found in Mid2p. On the other hand, there are a number of common elements. The amino-terminal portions of Mid1p and Mid2p contain a domain with significant similarity to the region of *Drosophila* anillin shown to directly bind and bundle actin filaments in vitro (Field and Alberts, 1995), although it remains to be determined whether or not either Mid1p or Mid2p interacts directly with actin filaments. Mid1p and Mid2p both contain PEST motifs conferring protein instability and similar carboxy-terminal regions that include a PH domain (~36%). Although PH domains can mediate the protein–phospholipid interactions necessary to localize proteins to the plasma membrane (for review see Lemmon and Ferguson, 2001), this region of Mid2p is not sufficient to direct GFP to the cell cortex nor is it required for Mid1p localization to the medial ring (this study; Paoletti and Chang, 2000). Moreover, the Mid2p PH domain lacks the consensus sequence that predicts direct and avid binding to phosphoinositides (Isakoff et al., 1998). Thus, the PH domains of these proteins may be involved in protein–protein interactions. In the case of Mid2p, this region is critical for its localization and function, and it is tempting to speculate that it mediates interaction with septins, a hypothesis currently being explored. In the case of Mid1p, the carboxy-terminal region including the PH domain is dispensable for its function (Paoletti and Chang, 2000). Thus, the amino terminus of Mid1p and the carboxy terminus of Mid2p are likely to be the key determinants in mediating their unique roles during cytokinesis.

As mentioned above, Mid1p and Mid2p share sequence similarity not only with each other but with human anillin. Interestingly, there are multiple uncharacterized anillin homologues in *Drosophila* and *C. elegans* (Oegema et al., 2000). The regions of particular sequence similarity include the possible actin-interacting region noted above and an ~200–amino acid stretch that includes the PH domain. Sequence alignments indicate that Mid1p (921 amino acids) is more similar to the larger anillin family members, such as Hs anillin (1,126 residues), *Drosophila* anillin (1201 residues), and the *C. elegans* gene product Y49E10.19 (1,205 residues). Conversely, Mid2p more closely resembles the smaller gene products, *C. elegans* Y43F8C.14 and *Drosophila* CG4530. Indeed, the characterized anillin family members in *Drosophila* and human seem to be more related to Mid1p than Mid2p in their localization pattern and loss of function phenotypes, with the exception of a connection to septins (Field and Alberts, 1995; Oegema et al., 2000). As these anillin homologues in higher eukaryotes are characterized, it will be interesting to learn whether they all function in cytokinesis. Further, it will be interesting to ascertain if they are functionally redundant or have distinct roles during cytokinesis as Mid1p and Mid2p do in *S. pombe*.

Several lines of evidence suggest that Mid2p affects septin ring organization and stability. In the absence of Mid2p, Spn3p–GFP is organized into a loose, rather than a tight, ring that disperses bilaterally across the septum as it forms. Conversely, in cells overproducing a stabilized Mid2p fragment, septin rings, or remnants thereof, persisted one to two cell divisions after they were formed. This observation implies that the turnover of full-length Mid2p might normally permit the timely disassembly of the septin ring. Furthermore, that these cells grew very slowly and were elongated upon the overproduction of nondegradable Mid2p indicates that septin ring disassembly may be important for normal cell cycle progression. In support of this possibility, cells producing a mutant form of the *S. cerevisiae* septin, Cdc3p, in which two Cdk sites have been altered to alanine, display two septin rings in G1 (Tang and Reed, 2002). Significantly, these cells are delayed in cell cycle progression until the old septin ring is disassembled (Tang and Reed, 2002).

In an independent study by Berlin et al. (2003), further evidence that Mid2p affects septin ring organization was obtained by FRAP analysis. The septin ring was found to be quite stable in wild-type cells, as assessed by the turnover of Spn4p–GFP (F. Chang, personal communication). In contrast, Spn4p–GFP was considerably more dynamic in *mid2Δ* cells, indicating that Mid2p function is required for the normal rigidity of the septin ring (F. Chang, personal communication).

Other anillin homologues have also been shown to influence septin ring organization. When *C. albicans* Int1p is overproduced in *S. cerevisiae*, highly ordered ectopic septin structures are observed in a manner strikingly similar to when Mid2p is overproduced (Gale et al., 2001). Further, overproduction of a carboxy-terminal fragment of Hs anillin induced the formation of ectopic septin containing structures with which Hs anillin was colocalized (Oegema et al., 2000). These abnormal cortical foci did not contain either actin or myosin-II (Oegema et al., 2000), nor did those formed upon Mid2p overproduction (Fig. 8 A; unpublished data). Thus, Mid2p shares with these proteins the ability to interfere with septin organization and function, although it is currently unknown whether the abnormal septin structures produced by Mid2p overproduction contain Mid2p.

An outstanding issue is how the events downstream of septation initiation network activation and septation are restricted temporally. Because all SCF targets identified to date are phosphorylated before being recognized by their cognate F-box protein (Willems et al., 1999), an appealing hypothesis is that the kinase that presumably modifies Mid2p in order to initiate its destruction might be conditionally activated upon the completion of septation. The identification of the protein kinase that phosphorylates Mid2p would significantly enhance our current understanding of the signaling pathways regulating cell separation.

Because Mid2p is only observed at the site of cell division, it follows then that the destruction machinery must also be recruited there. A candidate F-box protein is Pof6p, which was recently shown to localize to each side of the septum in dividing cells (Hermand et al., 2003). The loss of function of either Pof6p or the core SCF component Skp1p resulted

in aberrant or multiple septa, implying that elevated levels of certain factors may also inhibit efficient cell division (Hermand et al., 2003). Both the loss of the transcription factor Sep1p (Ribar et al., 1999) or a slight increase in its abundance generates a cell separation defect (unpublished data). Thus, the proper coordination of cytokinesis appears to require a fine balance between the activation and inhibition of various factors involved in the process.

The loss of function of a wide array of proteins in *S. pombe* produces similar cytokinesis defects. For example, deletion of the septins, calcineurin (Ppb1p), a transcription factor (Sep1p), a MAP kinase (Pmk1p), a MAP kinase phosphatase (Pmp1p), members of the exocyst complex (Sec6p), and now Mid2p all cause a long delay in the physical separation of cells after septum synthesis, although the nuclear cycle remains unaffected (J. Pringle, personal communication; Yoshida et al., 1994; Longtine et al., 1996; Toda et al., 1996; Sugiura et al., 1998; Ribar et al., 1999; Wang et al., 2002). Whereas septin ring disorganization is likely to be the underlying cause of the cell separation defect of *mid2Δ* cells, this is not the case for *ppb1Δ*. In *ppb1Δ* cells, both Spn3p–GFP and Mid2p–GFP localize normally. This result suggests that even though a number of mutants inhibit cell separation in *S. pombe*, defects in multiple pathways may lead to this phenotype. Determining how septin ring organization is affected in other cytokinesis mutants may help elucidate the pathways regulating cell separation.

Materials and methods

Strains, media, and methods

The *S. pombe* strains used in this study (Table I) were grown in YE or minimal medium with the appropriate supplements as previously described (Moreno et al., 1990). DNA transformations were done by electroporation (Prentice, 1992) or lithium acetate transformation (Keeney and Boeke, 1994). Induction of the *nmt* promoter (Basi et al., 1993; Maundrell, 1993) was achieved by growing cells in thiamine (promoter repressed) and then washing cells three times in medium lacking thiamine (promoter induced).

The *mid2*, *spn1*, and *spn3* ORFs were each tagged at their 3′ ends with either the *HA3-Kan*^{R}, myc13-Kan^R, or EGFP-Kan^R cassette, and the *spn3* ORF was also tagged with a *CFP-Kan*^{R} cassette as previously described (Bahler et al., 1998b). Kan^R transformants were screened by whole cell PCR and then by immunoblotting to confirm the accurate integration and expression of the fusion protein.

The *mid2*, *sep1*, and *spn4* ORFs were replaced with *ura4*$^+$ by homologous recombination in a diploid strain (Bahler et al., 1998b). Ura$^+$ transformants were screened for the proper gene disruptant by whole cell PCR. Heterozygous diploid strains were then sporulated at 25°C followed by tetrad dissection to determine if these genes were essential for viability.

Molecular biology techniques

PCR amplifications were performed with TaqPlus Precision polymerase (Stratagene) according to manufacturer's instructions. Oligonucleotides

Table I. **Strains used in this study**

Strain	Genotype	Source/reference
KGY246	*h*$^-$ *ade6-M210 ura4-D18 leu1-32*	Lab stock
KGY574	*h*$^-$ *mts3-1 leu1-32*	Lab stock
KGY1923	*h*$^-$ *cut2-myc::Kan*^{R} *mts3-1 leu1-32*	Berry et al., 1999
KGY1948	*h*$^-$ *cut2-myc::Kan*^{R} *mts3-1 lid1-6 ade6-M21X ura4-D18 leu1-32*	Berry et al., 1999
KGY1977	*h*$^-$*mid2-myc::Kan*^{R} *mts3-1 lid1-6 ade6-M21X ura4-D18 leu1-32*	This study
KGY1978	*h*$^+$ *mid2-myc::Kan*^{R} *mts3-1 skp1-A4 ade6-M21X ura4-D18 leu1-32*	This study
KGY2422	*h*$^-$ *mid2-GFP::Kan*^{R} *ade6-M210 ura4-D18 leu1-32*	This study
KGY2432	*h*$^-$ *mid2-myc::Kan*^{R} *ade6-M210 ura4-D18 leu1-32*	This study
KGY2843	*h*$^-$ *mid2-HA::Kan*^{R} *ade6-M210 ura4-D18 leu1-32*	This study
KGY2955	*h*$^-$ *mid1::ura4*$^+$ *ade6-M21X ura4-D18 leu1-32*	D. McCollum[a]
KGY3123	*h*$^+$ *mid2-GFP::Kan*^{R} *cdc25-22 ade6-M21X ura4-D18 leu1-32*	This study
KGY3125	*h*$^-$ *mid2::ura4*$^+$ *mid1::ura4*$^+$ *ade6-M21X ura4-D18 leu1-32*	This study
KGY3135	*h*$^-$ *mid2::ura4*$^+$ *ade6-M21X ura4-D18 leu1-32*	This study
KGY3244	*h*$^-$ *spn3-GFP::Kan*^{R} *ade6-M210 ura4-D18 leu1-32*	This study
KGY3295	*h*$^-$ *mid2-GFP::Kan*^{R} *spn1-CFP::Kan*^{R} *ade6-M210 ura4-D18 leu1-32*	This study
KGY3304	*h*$^+$ *spn3-GFP::Kan*^{R} *mid2::ura4*$^+$ *ade6-M21X ura4-D18 leu1-32*	This study
KGY3306	*h*$^-$ *mid2-HA::Kan*^{R} *cdc25-22 ade6-M21X ura4-D18 leu1-32*	This study
KGY3307	*h*$^-$ *mid2-HA::Kan*^{R} *mts3-1 ade6-M21X ura4-D18 leu1-32*	This study
KGY3419	*h*$^-$ *sep1::ura4*$^+$ *ade6-M21X ura4-D18 leu1-32*	This study
KGY3457	*h*$^+$ *mid2-HA::Kan*^{R} *sep1::ura4*$^+$ *cdc25-22 ade6-M21X ura4-D18 leu1-32*	This study
KGY3687	*h*$^+$ *mid2-myc::Kan*^{R} *mts3-1 ura4-D18 leu1-32*	This study
KGY3699	*h*^{90} *mid2-HA::Kan*^{R} *pop2::his7*$^+$ *ade6-M21X ura4-D18 his7-366 leu1-32*	This study
KGY3700	*h*^{90} *mid2-HA::Kan*^{R} *pop1::ura4*$^+$ *pop2::his7*$^+$ *ade6-M21X ura4-D18 his7-366 leu1-32*	This study
KGY3702	*h*^{90} *mid2-HA::Kan*^{R} *pop1::ura4*$^+$ *ura4-D18 leu1-32*	This study
KGY3986	*h*^{90} *spn4::ura4*$^+$ *ade6-M21X ura4-D18 leu1-32*	This study
KGY4050	*h*$^+$ *cut2-myc::Kan*^{R} *mts3-1 skp1-A4 ade6-M21X ura4-D18 leu1-32*	This study
KGY4062	*h*$^-$ *mid2::ura4*$^+$ *cdc25-22 ade6-M210 ura4-D18 leu1-32*	This study
KGY4216	*h*$^+$ *mid2-GFP::Kan*^{R} *ppb1::ura4*$^+$ *ade6-M210 ura4-D18 leu1-32*	This study
KGY4217	*h*^{90} *mid2-GFP::Kan*^{R} *spn4::ura4*$^+$ *ade6-M21X ura4-D18 leu1-32*	This study
KGY4220	*h*$^+$ *spn3-GFP::Kan*^{R} *ppb1::ura4*$^+$ *ade6-M210 ura4-D18 leu1-32*	This study
KGY4356	*h*$^+$ *mid2::ura4*$^+$ *spn4::ura4*$^+$ *ade6-M21X ura4-D18 leu1-32*	This study

[a]University of Massachusetts Medical School, Worcester, MA.

were synthesized by Integrated DNA Technologies, Inc., and all sequences are available upon request. Sequencing was done with Thermosequenase (USB) and Redivue ^{33}P Terminator Kit (Amersham Biosciences).

The entire *mid2* ORF was amplified from genomic DNA with oligos containing NdeI and BamHI sites on the 5′ and 3′ ends, respectively. The PCR product was cut with NdeI/BamHI and cloned into the thiamine-repressible pREP1, -41, -41HA, and -41GFP vectors to create pKG2207, pKG2208, pKG2491, and pKG2236. Primers containing 5′ NdeI/ATG and 3′ TAA/BamHI sites were also designed to amplify regions of Mid2p using pKG2208 as a template. These PCR products were also subcloned into the pREP series of vectors.

Cytology and microscopy

Strains producing GFP-tagged proteins were grown in YE medium, visualized live or fixed with ethanol or formaldehyde, and processed as previously described (Balasubramanian et al., 1997; Tomlin et al., 2002). To visualize cell walls, fixed cells were stained with aniline blue (methyl blue) (Sigma-Aldrich). Cells from a 1-ml culture were fixed in ethanol, resuspended in 1 ml of a 1:100 dilution of an aniline blue stock solution (100 mg/ml), incubated for 10 min, collected by centrifugation, washed three times with water, and resuspended in 20 μl water. LatA (Molecular Probes) was used at a concentration of 100 or 200 μM. Actin was visualized after formaldehyde fixation using AlexaFluor®594-phalloidin (Molecular Probes). Images were acquired digitally as previously described (Tomlin et al., 2002). For time-lapse experiments, cells were placed on a hanging drop glass slide (Fisher Scientific) containing solidified YE agar and covered with a coverslip. Time-lapse images of Spn3p–GFP and Mid2p–GFP were obtained using an Ultraview LCI confocal microscope equipped with a 488-nm Ar Ion laser (PerkinElmer). Images were captured using Ultraview LCI software (version 5.2; PerkinElmer) and processed using Velocity software (version 1.4.2; Improvision). Z-series optical sections were taken at 0.5-μm spacing at intervals of 2 or 3 min.

Immunoprecipitations and immunoblots

Whole cell lysates were prepared in NP-40 buffer followed by anti-HA or anti-Myc immunoprecipitations as previously described (Gould et al., 1991; McDonald et al., 1999). Denatured lysates were prepared as previously described (Burns et al., 2002). Protein samples were resolved on 4–12% NuPAGE gels in MOPS buffer and subsequently transferred to 0.2 μm nitrocellulose (Bio-Rad Laboratories) according to the manufacturer's instructions (Invitrogen). Immunoblotting was done with anti-HA (12CA5; 2 μg/ml), anti-Myc (9E10; 2 μg/ml), anti-Cdc13p (GJG56; 1:2,500 of serum), anti-Cdc2p (PSTAIRE; 1:5,000; Sigma-Aldrich), or anti-ubiquitin (1:100; Sigma-Aldrich). The primary antibodies were detected with HRP-conjugated goat anti–mouse or goat anti–rabbit secondary antibodies (0.4 mg/ml; Jackson ImmunoResearch Laboratories) at a dilution of 1:50,000 followed by ECL visualization using SuperSignal (Pierce Chemical Co.).

Immunoprecipitation/phosphatase assay

After an anti-HA immunoprecipitation from denatured lysate, beads were washed two times with 1 ml NP-40 buffer, four times with 1 ml of phosphatase buffer (25 mM Hepes-NaOH, pH 7.4, 150 mM NaCl, 0.1 mg/ml BSA), divided in half, pulsed down, and the supernatant aspirated off. 10-μl reactions composed of 1X phosphatase buffer, 2 mM $MnCl_2$, plus 1 μl of λ-phosphatase (New England Biolabs, Inc.) or 1 μl H_2O were then incubated at 30°C for 45 min with gentle mixing every 5 min. The beads were washed three times with NP-40 buffer and resuspended in 25 μl 2X lithium dodecyl sulfate sample buffer.

Northern blotting

Total RNA was prepared by extraction with hot acidic phenol and SDS as detailed previously (Burns et al., 1999). Total RNA (20 μg per sample) was resolved on formaldehyde-agarose gels and capillary blotted to a Duralon-UV membrane. *mid2*$^+$ and *his3*$^+$ mRNA levels were detected by hybridization of ^{32}P-labeled oligonucleotide probes (Rediprime II; Amersham Biosciences) from regions within their ORFs. The blots were exposed to Phosphor-Imager screens and visualized with ImageQuant 5.2 on an Amersham Biosciences Typhoon 9200 scanner.

In vivo ubiquitination assays

Strains carrying pREP1-His_6–ubiquitin were grown at 25°C for 22 h in the absence of thiamine to induce the expression of His_6–ubiquitin (Ub), shifted to 36°C for 4 h, and then 6×10^8 cells were harvested. Cell lysates were prepared in the presence of 8 M urea with 100 mM sodium phosphate, pH 8.0, and 5 mM imidazole followed by binding of His_6–Ub-conjugated proteins to a nickel affinity resin (Ni-NTA Superflow; QIAGEN). The beads were washed as previously described (Benito et al., 1998) and ubiquitinated proteins eluted with 200 mM imidazole.

Online supplemental material

The supplemental material for this article is available at http://www.jcb.org/cgi/content/full/jcb.200211126/DC1. Three Quicktime movie files of the following live cells are available online: Mid2p–GFP (Video 1), Spn3p-GFP (Video 2), and Spn3p-GFP in a *mid2Δ* strain (Video 3).

The authors wish to thank F. Chang (Columbia University, New York, NY) and J. Pringle (University of North Carolina at Chapel Hill, Chapel Hill, NC) for communicating results prior to publication, T. Toda (Imperial Cancer Research Fund, London, UK) for providing strains, G. Burns, A. Feoktistova, and L. Pundor for excellent technical advice and assistance, and J. Pringle for providing *spn* null strains that prompted our study of the relationship between Mid2p and septins as well as for helpful comments on the manuscript.

J.J. Tasto was supported by National Institutes of Health grant T32GM08554. This work was supported by the Howard Hughes Medical Institute of which K.L. Gould is an associate investigator.

Submitted: 26 November 2002
Revised: 13 February 2003
Accepted: 25 February 2003

References

Alfa, C.E., R. Booher, D. Beach, and J.S. Hyams. 1989. Fission yeast cyclin: subcellular localisation and cell cycle regulation. *J. Cell Sci. Suppl.* 12:9–19.

Ayscough, K.R., J. Stryker, N. Pokala, M. Sanders, P. Crews, and D.G. Drubin. 1997. High rates of actin filament turnover in budding yeast and roles for actin in establishment and maintenance of cell polarity revealed using the actin inhibitor latrunculin-A. *J. Cell Biol.* 137:399–416.

Bahler, J., A.B. Steever, S. Wheatley, Y. Wang, J.R. Pringle, K.L. Gould, and D. McCollum. 1998a. Role of polo kinase and Mid1p in determining the site of cell division in fission yeast. *J. Cell Biol.* 143:1603–1616.

Bahler, J., J.Q. Wu, M.S. Longtine, N.G. Shah, A. McKenzie III, A.B. Steever, A. Wach, P. Philippsen, and J.R. Pringle. 1998b. Heterologous modules for efficient and versatile PCR-based gene targeting in *Schizosaccharomyces pombe*. *Yeast.* 14:943–951.

Balasubramanian, M.K., D. McCollum, and K.L. Gould. 1997. Cytokinesis in fission yeast *Schizosaccharomyces pombe*. *Methods Enzymol.* 283:494–506.

Basi, G., E. Schmid, and K. Maundrell. 1993. TATA box mutations in the *Schizosaccharomyces pombe* nmt1 promoter affect transcription efficiency but not the transcription start point or thiamine repressibility. *Gene.* 123:131–136.

Benito, J., C. Martin-Castellanos, and S. Moreno. 1998. Regulation of the G1 phase of the cell cycle by periodic stabilization and degradation of the p25rum1 CDK inhibitor. *EMBO J.* 17:482–497.

Berlin, A., A. Paoletti, and F. Chang. 2003. Mid2p stabilizes septin rings during cytokinesis in fission yeast. *J. Cell Biol.* 160:1083–1092.

Berry, L.D., A. Feoktistova, M.D. Wright, and K.L. Gould. 1999. The *Schizosaccharomyces pombe dim1*(+) gene interacts with the anaphase-promoting complex or cyclosome (APC/C) component *lid1*(+) and is required for APC/C function. *Mol. Cell. Biol.* 19:2535–2546.

Burns, C.G., R. Ohi, A.R. Krainer, and K.L. Gould. 1999. Evidence that Myb-related CDC5 proteins are required for pre-mRNA splicing. *Proc. Natl. Acad. Sci. USA.* 96:13789–13794.

Burns, C.G., R. Ohi, S. Mehta, E.T. O'Toole, M. Winey, T.A. Clark, C.W. Sugnet, M. Ares, Jr., and K.L. Gould. 2002. Removal of a single α-tubulin gene intron suppresses cell cycle arrest phenotypes of splicing factor mutations in *Saccharomyces cerevisiae*. *Mol. Cell. Biol.* 22:801–815.

Chang, F. 2001. Studies in fission yeast on mechanisms of cell division site placement. *Cell Struct. Funct.* 26:539–544.

Chang, F., A. Woollard, and P. Nurse. 1996. Isolation and characterization of fission yeast mutants defective in the assembly and placement of the contractile actin ring. *J. Cell Sci.* 109(Pt 1):131–142.

Faty, M., M. Fink, and Y. Barral. 2002. Septins: a ring to part mother and daughter. *Curr. Genet.* 41:123–131.

Feierbach, B., and F. Chang. 2001. Cytokinesis and the contractile ring in fission yeast. *Curr. Opin. Microbiol.* 4:713–719.

Field, C.M., and B.M. Alberts. 1995. Anillin, a contractile ring protein that cycles

from the nucleus to the cell cortex. *J. Cell Biol.* 131:165–178.

Gale, C., D. Finkel, N. Tao, M. Meinke, M. McClellan, J. Olson, K. Kendrick, and M. Hostetter. 1996. Cloning and expression of a gene encoding an integrin-like protein in *Candida albicans*. *Proc. Natl. Acad. Sci. USA.* 93:357–361.

Gale, C., M. Gerami-Nejad, M. McClellan, S. Vandoninck, M.S. Longtine, and J. Berman. 2001. *Candida albicans* Int1p interacts with the septin ring in yeast and hyphal cells. *Mol. Biol. Cell.* 12:3538–3549.

Gladfelter, A.S., J.R. Pringle, and D.J. Lew. 2001. The septin cortex at the yeast mother-bud neck. *Curr. Opin. Microbiol.* 4:681–689.

Gordon, C., G. McGurk, M. Wallace, and N.D. Hastie. 1996. A conditional lethal mutant in the fission yeast 26 S protease subunit *mts3+* is defective in metaphase to anaphase transition. *J. Biol. Chem.* 271:5704–5711.

Gould, K.L., S. Moreno, D.J. Owen, S. Sazer, and P. Nurse. 1991. Phosphorylation at Thr167 is required for *Schizosaccharomyces pombe* p34cdc2 function. *EMBO J.* 10:3297–3309.

Hartwell, L.H. 1971. Genetic control of the cell division cycle in yeast. IV. Genes controlling bud emergence and cytokinesis. *Exp. Cell Res.* 69:265–276.

Hermand, D., S. Bamps, L. Tafforeau, J. Vandenhaute, and T.P. Makela. 2003. Skp1 and the F-box protein Pof6 are essential for cell separation in fission yeast. *J. Biol. Chem.* 278:9671–9677.

Isakoff, S.J., T. Cardozo, J. Andreev, Z. Li, K.M. Ferguson, R. Abagyan, M.A. Lemmon, A. Aronheim, and E.Y. Skolnik. 1998. Identification and analysis of PH domain-containing targets of phosphatidylinositol 3-kinase using a novel in vivo assay in yeast. *EMBO J.* 17:5374–5387.

Keeney, J.B., and J.D. Boeke. 1994. Efficient targeted integration at *leu1-32* and *ura4-294* in *Schizosaccharomyces pombe*. *Genetics.* 136:849–856.

Kinoshita, M., S. Kumar, A. Mizoguchi, C. Ide, A. Kinoshita, T. Haraguchi, Y. Hiraoka, and M. Noda. 1997. Nedd5, a mammalian septin, is a novel cytoskeletal component interacting with actin-based structures. *Genes Dev.* 11: 1535–1547.

Kinoshita, M., C.M. Field, M.L. Coughlin, A.F. Straight, and T.J. Mitchison. 2002. Self- and actin-templated assembly of mammalian septins. *Dev. Cell.* 3:791–802.

Kominami, K., I. Ochotorena, and T. Toda. 1998. Two F-box/WD-repeat proteins Pop1 and Pop2 form hetero- and homo-complexes together with cullin-1 in the fission yeast SCF (Skp1-Cullin-1-F-box) ubiquitin ligase. *Genes Cells.* 3:721–735.

Krek, W. 1998. Proteolysis and the G1-S transition: the SCF connection. *Curr. Opin. Genet. Dev.* 8:36–42.

Le Goff, X., S. Utzig, and V. Simanis. 1999. Controlling septation in fission yeast: finding the middle, and timing it right. *Curr. Genet.* 35:571–584.

Lemmon, M.A., and K.M. Ferguson. 2001. Molecular determinants in pleckstrin homology domains that allow specific recognition of phosphoinositides. *Biochem. Soc. Trans.* 29:377–384.

Longtine, M.S., D.J. DeMarini, M.L. Valencik, O.S. Al-Awar, H. Fares, C. De Virgilio, and J.R. Pringle. 1996. The septins: roles in cytokinesis and other processes. *Curr. Opin. Cell Biol.* 8:106–119.

Macara, I.G., R. Baldarelli, C.M. Field, M. Glotzer, Y. Hayashi, S.C. Hsu, M.B. Kennedy, M. Kinoshita, M. Longtine, C. Low, et al. 2002. Mammalian septins nomenclature. *Mol. Biol. Cell.* 13:4111–4113.

Maundrell, K. 1993. Thiamine-repressible expression vectors pREP and pRIP for fission yeast. *Gene.* 123:127–130.

McCollum, D., and K.L. Gould. 2001. Timing is everything: regulation of mitotic exit and cytokinesis by the MEN and SIN. *Trends Cell Biol.* 11:89–95.

McDonald, W.H., R. Ohi, N. Smelkova, D. Frendewey, and K.L. Gould. 1999. Myb-related fission yeast cdc5p is a component of a 40S snRNP-containing complex and is essential for pre-mRNA splicing. *Mol. Cell. Biol.* 19:5352–5362.

Moreno, S., P. Nurse, and P. Russell. 1990. Regulation of mitosis by cyclic accumulation of p80cdc25 mitotic inducer in fission yeast. *Nature.* 344:549–552.

Neufeld, T.P., and G.M. Rubin. 1994. The *Drosophila* peanut gene is required for cytokinesis and encodes a protein similar to yeast putative bud neck filament proteins. *Cell.* 77:371–379.

Oegema, K., M.S. Savoian, T.J. Mitchison, and C.M. Field. 2000. Functional analysis of a human homologue of the *Drosophila* actin binding protein anillin suggests a role in cytokinesis. *J. Cell Biol.* 150:539–552.

Paoletti, A., and F. Chang. 2000. Analysis of mid1p, a protein required for placement of the cell division site, reveals a link between the nucleus and the cell surface in fission yeast. *Mol. Biol. Cell.* 11:2757–2773.

Pereira, G., and E. Schiebel. 2001. The role of the yeast spindle pole body and the mammalian centrosome in regulating late mitotic events. *Curr. Opin. Cell Biol.* 13:762–769.

Peters, J.M. 2002. The anaphase-promoting complex: proteolysis in mitosis and beyond. *Mol. Cell.* 9:931–943.

Prentice, H.L. 1992. High efficiency transformation of *Schizosaccharomyces pombe* by electroporation. *Nucleic Acids Res.* 20:621.

Ribar, B., A. Grallert, E. Olah, and Z. Szallasi. 1999. Deletion of the *sep1*(+) forkhead transcription factor homologue is not lethal but causes hyphal growth in *Schizosaccharomyces pombe*. *Biochem. Biophys. Res. Commun.* 263:465–474.

Rogers, S., R. Wells, and M. Rechsteiner. 1986. Amino acid sequences common to rapidly degraded proteins: the PEST hypothesis. *Science.* 234:364–368.

Sanders, S.L., and I. Herskowitz. 1996. The BUD4 protein of yeast, required for axial budding, is localized to the mother/BUD neck in a cell cycle–dependent manner. *J. Cell Biol.* 134:413–427.

Sohrmann, M., C. Fankhauser, C. Brodbeck, and V. Simanis. 1996. The *dmf1/mid1* gene is essential for correct positioning of the division septum in fission yeast. *Genes Dev.* 10:2707–2719.

Sugiura, R., T. Toda, H. Shuntoh, M. Yanagida, and T. Kuno. 1998. *pmp1+*, a suppressor of calcineurin deficiency, encodes a novel MAP kinase phosphatase in fission yeast. *EMBO J.* 17:140–148.

Tang, C.S., and S.I. Reed. 2002. Phosphorylation of the septin cdc3 in g1 by the cdc28 kinase is essential for efficient septin ring disassembly. *Cell Cycle.* 1:42–49.

Toda, T., S. Dhut, G. Superti-Furga, Y. Gotoh, E. Nishida, R. Sugiura, and T. Kuno. 1996. The fission yeast *pmk1+* gene encodes a novel mitogen-activated protein kinase homolog which regulates cell integrity and functions coordinately with the protein kinase C pathway. *Mol. Cell. Biol.* 16:6752–6764.

Tomlin, G.C., J.L. Morrell, and K.L. Gould. 2002. The spindle pole body protein Cdc11p links Sid4p to the fission yeast septation initiation network. *Mol. Biol. Cell.* 13:1203–1214.

Wang, H., X. Tang, J. Liu, S. Trautmann, D. Balasundaram, D. McCollum, and M.K. Balasubramanian. 2002. The multiprotein exocyst complex is essential for cell separation in *Schizosaccharomyces pombe*. *Mol. Biol. Cell.* 13:515–529.

Willems, A.R., T. Goh, L. Taylor, I. Chernushevich, A. Shevchenko, and M. Tyers. 1999. SCF ubiquitin protein ligases and phosphorylation-dependent proteolysis. *Philos. Trans. R. Soc. Lond. B Biol. Sci.* 354:1533–1550.

Yamano, H., K. Kitamura, K. Kominami, A. Lehmann, S. Katayama, T. Hunt, and T. Toda. 2000. The spike of S phase cyclin Cig2 expression at the G1-S border in fission yeast requires both APC and SCF ubiquitin ligases. *Mol. Cell.* 6:1377–1387.

Yoshida, T., T. Toda, and M. Yanagida. 1994. A calcineurin-like gene *ppb1+* in fission yeast: mutant defects in cytokinesis, cell polarity, mating and spindle pole body positioning. *J. Cell Sci.* 107(Pt 7):1725–1735.

Zachariae, W., and K. Nasmyth. 1999. Whose end is destruction: cell division and the anaphase-promoting complex. *Genes Dev.* 13:2039–2058.